Supplementary Material for: **Temperature-dependent spectral emission of hexagonal boron nitride quantum emitters on conductive and dielectric substrates**

Hamidreza Akbari[1], Wei-Hsiang Lin[1], Benjamin Vest[1,2], Pankaj K. Jha[1], Harry A. Atwater[1]

[1]Thomas J. Watson laboratory of applied physics, California Institute of Technology, Pasadena, CA., 91106

[2] Université Paris-Saclay, Institut d'Optique Graduate School, CNRS, Laboratoire Charles Fabry, 91127, Palaiseau, France.

Material and Sample preparation

Bulk hBN preparation: h-BN crystals (HQ graphene) were exfoliated via mechanical exfoliation with scotch tape onto 300nm SiO_2 on Si substrate (MTI Corp.). Then the sample was annealed at 850C for 30 minutes under Argon at room pressure.

CVD hBN preparation: CVD hBN was grown by the method described in our previous work [1] and transferred via polymer assisted wet transfer technique [1] onto SiO_2 on Si (MTI Corp.) and ITO on Si substrate. No post processing was performed on CVD hBN to activate emitters.

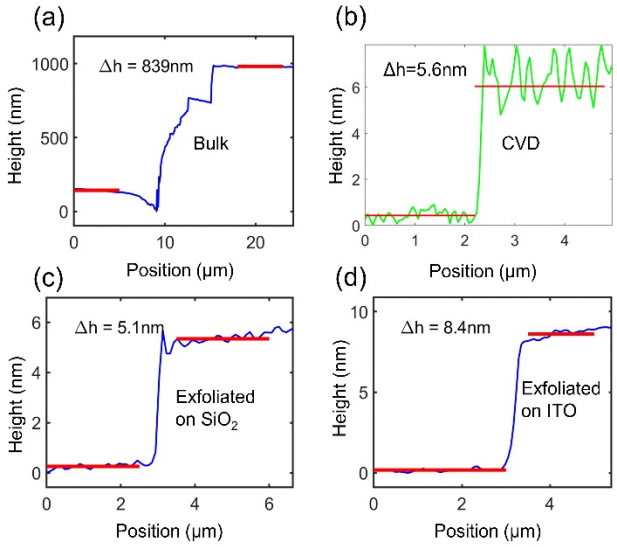

Figure S-1. AFM measurement result of Bulk, CVD, and exfoliated flakes used for this study.

Exfoliated hBN preparation: an hBN crystal was annealed at 900C for 30 minutes under Argon environment and then flakes were exfoliated via mechanical exfoliation with scotch tape onto 300nm SiO_2 on Si substrate and ITO on Si substrate.

The thickness of hBN was measured using Asylum Research Atomic Force Microscope (AFM).

The ITO film is deposited via room-temperature RF magnetron sputtering on top of Si substrate. The deposition pressure is 3 mTorr and the applied RF power is 48W. The plasma is struck by using Argon gas with a flow rate of 20 SCCM, and Argon/Oxygen mixture gas with ratio 90/10 with a flow rate of 0.6 SCCM is used to control the resistance of the deposited layer. The thickness of ITO Film is 50nm.

Experiment Setup

Room temperature characterization was done with a homebuilt confocal microscope.

Emitters were pumped with a 100 μW beam of 532nm laser (Cobolt). Linearly polarized laser was passed through a quarter wave plate oriented at 45 degrees relative to the polarization axis to produce a circularly polarized light, we used circularly polarized light for excitation to excite all dipole emitters irrespective of their in-plane dipole orientation. Mapping was done with a Newport fast scanning mirror.

a 100X (NA=0.95) Leica objective was used to focus the light on the sample and a tunable bandpass filter (Semrock Versa-chrome) was used to pass ZPL and we used a grating-based spectrometer (Princeton Instruments HRS300) to measure spectra. Low-temperature spectroscopy was performed with an attocube attodry800 system. The sample holder stage was cooled by circulating liquid He. The sample was mounted on the cooled piezo stage using Apiezon thermal grease. A low-temperature attocube objective was used to focus 532nm fiber-coupled laser (PicoQuant) on the sample.

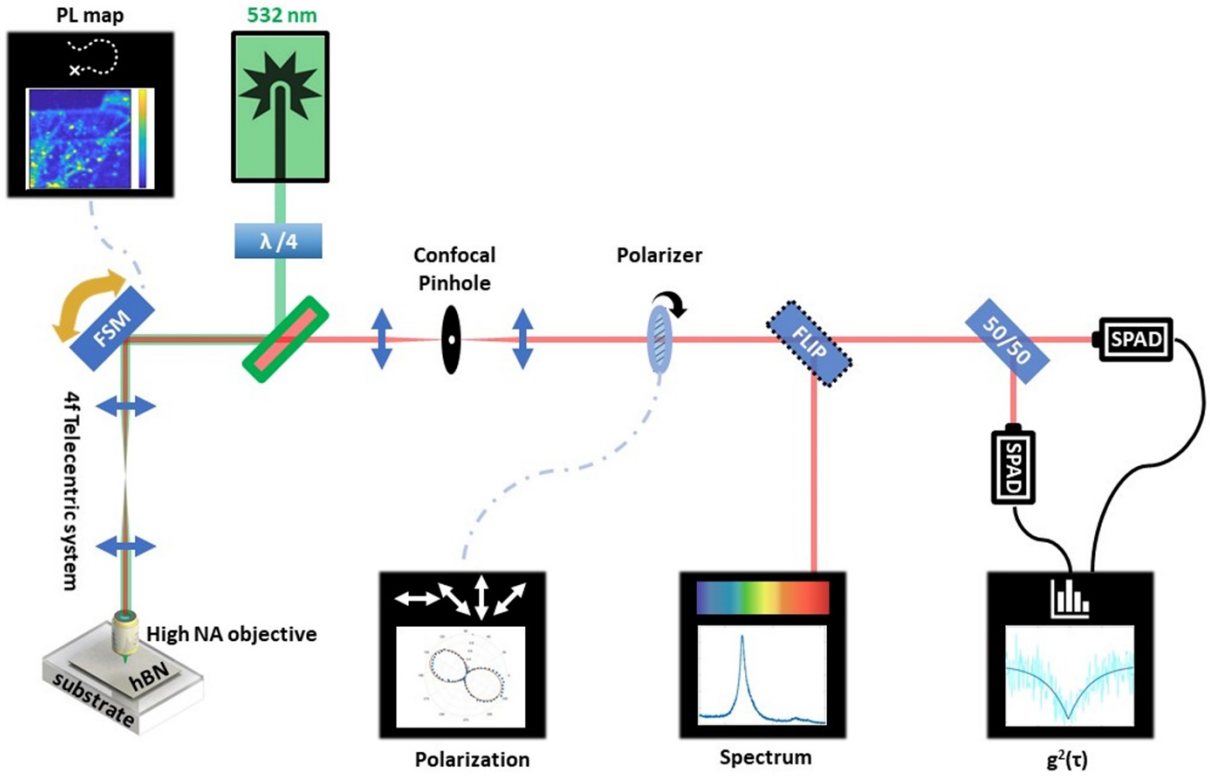

Figure S-2. Schematic of homebuilt confocal microscope

We used a Raman spectrometer (Princeton instruments HRS750 spectrograph with 2400 g/mm grating) to measure PL with spectral resolution of 0.007nm at 532 nm Spectral resolution was measured by measuring linewidth of the 532nm laser.

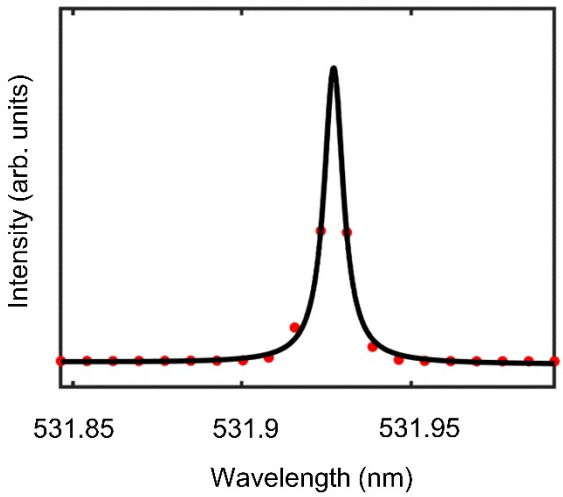

Figure S-3. Spectral resolution of the spectrometer

Polarization measurement shown in figure S-4 was done by adding a wire grid polarizer (Thorlabs Inc.) before the light enters the beam splitter of HBT setup and inputs of two APDs were integrated to calculate signal.

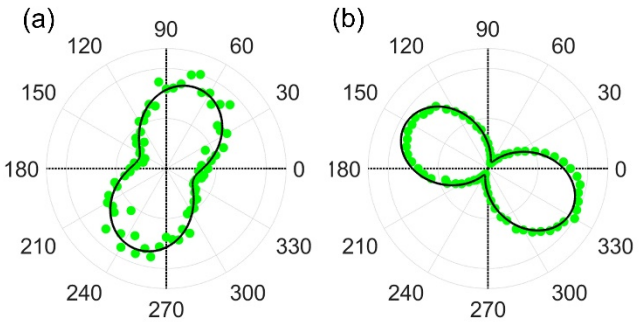

Figure S-4. Polarimetry result of two emitters. Emitter 1 (left) shows some out of plane component and emitter 2 (right) shows almost completely in-plane dipole signature

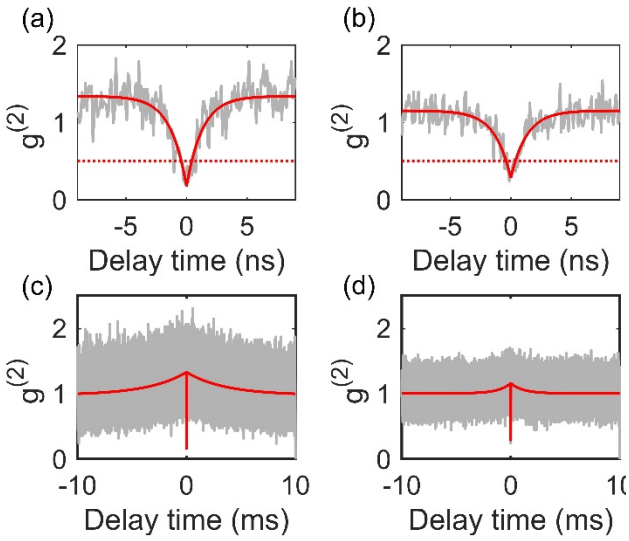

Figure S-5. result of photon intensity autocorrelation measurement($g^{(2)}$)

Two avalanche photodiodes (PicoQuant) were used to measure autocorrelation and a picoharp-300 module was used to register photon events in TTTR mode. g^2 data were analyzed with a custom MATLAB script and the result is shown in figure S-5.

Low frequency spectral diffusion

Low frequency spectral diffusion (spectral diffusion for time scales larger than 1 minute) of the two emitters discussed in the main manuscript is shown in Figure S-6.

Each spectrum was acquired using 100μW laser power (measured before objective) and data acquisition time of 1 minute. For spectral stability measurements, 120 consecutive spectra were measured each for 1 minute. We also fitted data of each instant with Voigt function to extract the position of the peak and compared the position of the peak with mean FWHM of the spectral line. furthermore, we performed a Fourier transform on the trajectory of peak in time to extract frequency spectrum of spectral diffusion

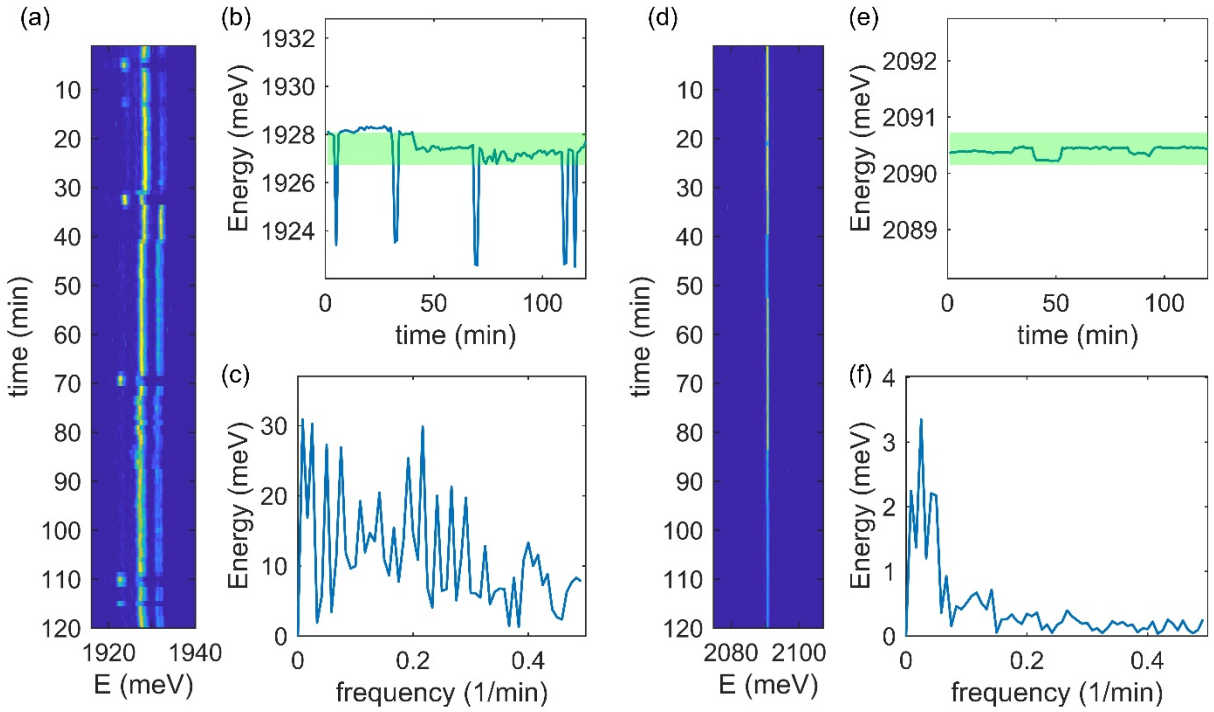

Figure S-6. Low-frequency spectral diffusion signature of emitters. (a) shows spectral diffusion of emitter 1 for 120 minutes, (b) shows the position of ZPL peak at each time and (c) is Fourier transform of (b). Panels (d),(e) and (f) show similar results for emitter 2. The shaded region in (b) and (e) specifies the FWHM of each emitter.

Average amplitude of Fourier transform of slow spectral diffusion (w) of each emitter as a function of inhomogeneous linewidth is plotted in Figure S-7.

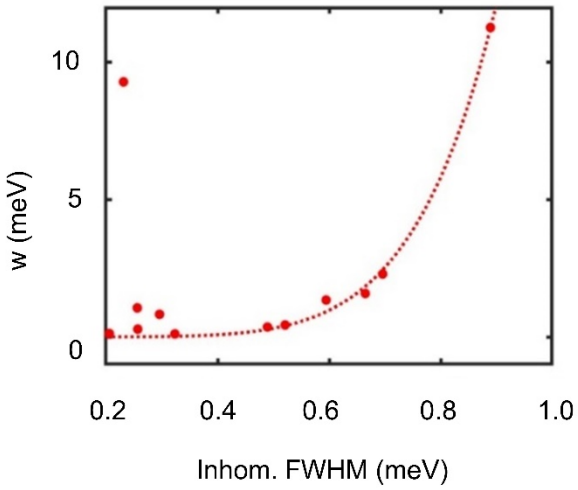

Figure S-7. Correlation between average Amplitude of low frequency spectral diffusion and Inhomogeneous FWHM at 4K for 12 emitters in bulk hBN

Except for one data point which corresponds to a defect with narrow inhomogeneous linewidth and strong spectral jumps the general trend shows increase of spectral diffusion as linewidth increases. We attribute this behavior to the similar nature of low frequency spectral diffusion which results in spectral jumps in Fig. S-6 and high frequency spectral diffusion which results in broadening of ZPL

Blinking Analysis

In Fig S-8, we have plotted the count rate of photons as a function of time for emitters A and B and we analyzed the blinking of these two emitters. we plotted histogram of blinking (OFF) time for both emitters and as can be seen emitter 1 has higher probability of longer blinking times compared to emitter 2. This behavior is consistent with longer T_2 from $g^{(2)}(t)$ fit (See Fig. S-5) considering that the origin of blinking is shelving in the metastable state.

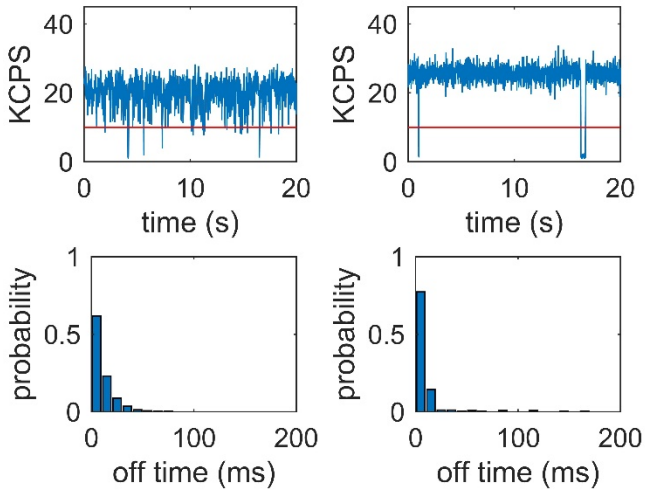

Figure S-8. count rate of detected photons from emitter 1 (a) and emitter 2(b) plotted for 20 seconds. The red line at 10 kcps is the threshold of ON/OFF states. The duration of blinks(duration of off times) are extracted for 2000 second total experiment time and its normalized histogram is shown in (c)for emitter 1 and in (d) for emitter 2.

Spectral data of emitters

For the emitters shown in the figure 5 of the manuscript the full ZPL profile is shown in Figure S-9. To extract FWHM of these peaks, if more than one peak was present we perform the fitting with multiple Voigt profiles and the FWHM was considered to be the FWHM of the Voigt profile with largest amplitude (the main peak). Also $g^{(2)}(t)$ data for these 4 emitters is plotted in Fig. S-9 (e-f) and no correlation between the parameters of $g^{(2)}$ plot and substrate/hBN was not detected.

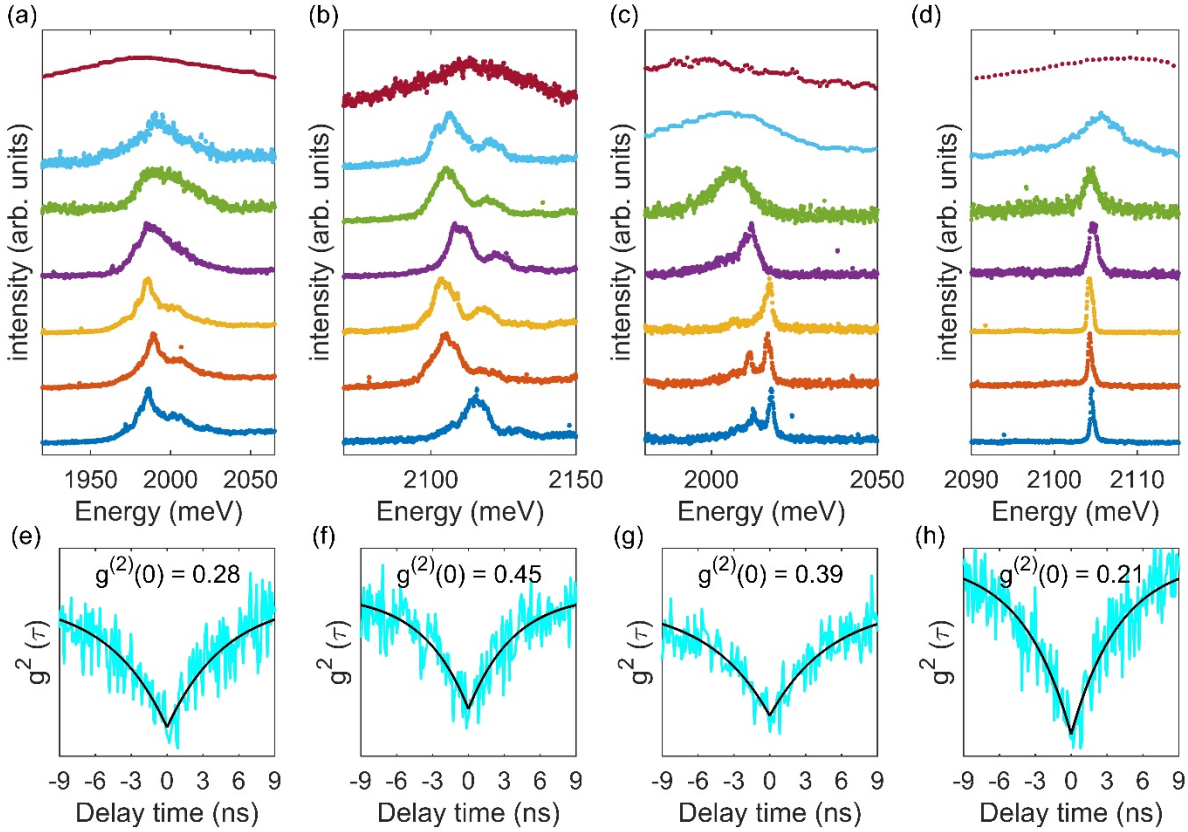

Figure S-9. evolution of ZPL linewidth with temperature for emitters at 4K,10K,20K,40K,80K,160K,300K (from bottom to top) for (a) emitter in CVD hBN atop SiO_2 (b) emitter in CVD hBN atop ITO, (c) emitter in exfoliated hBN atop SiO_2 and (d) emitter in exfoliated hBN atop ITO , (e-f) represent $g^{(2)}$ result for these emitters.

References:

[1] W. H. Lin, V. W. Brar, D. Jariwala, M. C. Sherrott, W. S. Tseng, C. I. Wu, N. C. Yeh, and H. A. Atwater, *Atomic-Scale Structural and Chemical Characterization of Hexagonal Boron Nitride Layers Synthesized at the Wafer-Scale with Monolayer Thickness Control*, Chem. Mater. **29**, 4700 (2017).